

# Understanding focus effects in submicrometer optical lithography: a review

Chris A. Mack, MEMBER SPIE  
FINLE Technologies  
P.O. Box 162712  
Austin, Texas 78716

**Abstract.** A review is presented on focus effects in optical lithography. Alternative definitions of resolution and depth of focus are given based on an understanding of the interactions of the aerial image with the photoresist process. This interaction points to various aspects of the aerial image that are important from a lithographic point of view, especially the aerial image log-slope. The effects of numerical aperture, wavelength, feature size, and feature type can also be characterized using the log-slope defocus curve, thereby permitting objective comparisons of different lithographic tools. The impact of the photoresist on the response of the process to changes in focus is described as two major effects. First, improving the photoresist results in improved exposure latitude. This in turn allows the image to be further degraded by focus errors and still give acceptable results. Second, submicrometer optical lithography usually results in asymmetrical focus behavior because of the defocusing of the aerial image as it propagates through the photoresist. Finally, several methods for depth-of-focus improvement are discussed and their relative merits and drawbacks are reviewed.

*Subject terms:* microlithography; optical lithography; depth of focus.  
*Optical Engineering* 32(10), 2350–2362 (October 1993).

## 1 Introduction

In the age of submicrometer optical lithography, focus has become a critical process parameter. Each decrease in minimum feature size is accompanied by a corresponding decrease in depth of focus (DOF). However, sources of focus errors, such as wafer nonflatness, topography, and the ability to determine best focus, are not being reduced in proportion to the DOF. Thus, the effects of focus on the practical resolution capabilities of a lithographic tool are becoming increasingly important.

In describing the resolution and depth of focus of a lithographic system, it is common to apply the Rayleigh criteria. The Rayleigh criterion for the minimum resolvable feature size  $R$  is

$$R = k_1 \frac{\lambda}{NA}, \quad (1)$$

where  $\lambda$  is the exposure wavelength,  $NA$  is the numerical aperture of the objective lens, and  $k_1$  is referred to as a “pro-

cess-dependent constant” and is typically quoted in the range of 0.4 to 0.9. Similarly, the Rayleigh DOF is given by

$$DOF = k_2 \frac{\lambda}{NA^2}, \quad (2)$$

where  $k_2$  is another process-dependent constant with values typically in the range of 0.5 to 1.0.

In the submicrometer imaging regime, the simple Rayleigh criteria are not adequate for describing the resolution and depth of focus of a microlithographic process. In fact, the common characterization of  $k_1$  and  $k_2$  as constants leads to many misinterpretations of these equations. A more appropriate way to view the Rayleigh criteria are as scaling equations. Resolution scales as  $\lambda/NA$ , so  $k_1$  is, in fact, the scaled resolution. Similarly, the DOF scales as  $\lambda/NA^2$ , so  $k_2$  is the scaled DOF. The scaled quantities  $k_1$  and  $k_2$  are not constants and vary greatly as a function of many lithographic parameters. The Rayleigh equations give no information about the values of  $k_1$  and  $k_2$ , their interdependence, or their dependence on other parameters.

In this paper, a previously published series of papers on focus effects in optical lithography is reviewed.<sup>1–4</sup> Alternative definitions of resolution and depth of focus are given based on an understanding of the interactions of the aerial image with the photoresist process. This interaction points to various aspects of the aerial image that are important from

Paper MIC-16 received April 12, 1993; revised manuscript received May 14, 1993; accepted for publication May 24, 1993. This paper is a revision of three papers presented at the SPIE conferences on Optical/Laser Microlithography I, II, and V, March 1988, Santa Clara, Calif., and March 1989 and 1992, San Jose, Calif. The papers presented there appear (unrefereed) in SPIE Proceedings Vols. 922, 1088, and 1674.  
© 1993 Society of Photo-Optical Instrumentation Engineers. 0091-3286/93/\$6.00.

a lithographic point of view. Defining a physically significant metric of aerial image quality allows one to characterize the effects of feature size and focus and leads to new definitions for resolution and DOF. The effects of numerical aperture, wavelength, feature size, and feature type can also be characterized using this technique, thereby permitting objective comparisons of different lithographic tools.

Photoresist can have a major impact on the response of the process to changes in focus. First, improving the photoresist results in improved exposure latitude. This in turn allows the image to be further degraded by focus errors and still give acceptable results. Second, submicrometer optical lithography usually results in asymmetrical focus behavior because of the defocusing of the aerial image as it propagates through the photoresist. Both of these effects are discussed in this paper.

Finally, several methods for depth-of-focus improvement are discussed and their relative merits and drawbacks are reviewed.

## 2 Aerial Image

To simplify the analysis of a lithographic process, it is highly desirable to separate the effects of the lithographic tool from those of the photoresist process. This can be done with reasonable accuracy only if the interaction of the tool (i.e., the aerial image) with the photoresist is known. Consider an aerial image of relative intensity  $I(x)$ , where  $x$  is the horizontal position (i.e., in the plane of the wafer and mask) and is zero at the center of a symmetric mask feature. The aerial image exposes the photoresist to produce some chemical distribution  $m(x)$  within the resist. This distribution is called the latent image. Many important properties of the lithographic process, such as exposure latitude and development latitude, are a function of the gradient of the latent image  $\partial m/\partial x$ . Larger gradients result in improved process latitude. It has been shown that the latent image gradient is related to the aerial image by<sup>5</sup>

$$\frac{\partial m}{\partial x} = m \ln(m) \frac{\partial \ln I}{\partial x}, \quad (3)$$

where the logarithmic slope of the aerial image is often called just the log-slope. The development properties of the photoresist translate the latent image gradient into a development gradient, which then allows for the generation of a photoresist image. Optimum photoresist image quality is obtained with a large development rate gradient. A lumped parameter called the photoresist contrast  $\gamma$  can be defined that relates the aerial image and the development rate  $r$  (see Appendix A for a derivation):

$$\frac{\partial \ln r}{\partial x} = \gamma \frac{\partial \ln I}{\partial x}. \quad (4)$$

Equation (4) is called the lithographic imaging equation and shows in a concise form how a gradient in aerial image intensity results in a solubility differential in photoresist. The development rate gradient is maximized by higher resist contrast and by a larger log-slope of the aerial image.

The preceding discussion clearly indicates that the aerial image log-slope is a logical metric by which to judge the quality of the aerial image. In particular, the image log-slope,

when normalized by multiplying by the feature width, is directly proportional to exposure latitude expressed as a percent change in exposure to give a percent change in linewidth. This normalized log-slope (NLS) is given by

$$\text{NLS} = w \frac{\partial \ln I}{\partial x}. \quad (5)$$

This metric was first discussed by Levenson et al.<sup>6</sup> and later, in a related form, by Levinson and Arnold,<sup>7,8</sup> before being explored to great extent by this author.<sup>1-4</sup>

## 3 Focus and the Aerial Image

Shown in Fig. 1 is the well-known effect of defocus on the aerial image. Both the edge slope of the image and the center intensity decrease with defocus, and the intensity at the mask edge remains nearly constant or increases slightly. To compare aerial images using the log-slope, one must pick an  $x$  value to use. An obvious choice is the mask edge (or more correctly, the nominal feature edge). Thus, all subsequent reference to the slope of the log-aerial image are at the nominal feature edge. Now the effect of defocus on the aerial image can be expressed by plotting log-slope as a function of defocus, as shown in Fig. 2. The log-slope defocus curve has proven to be a powerful tool for understanding focus effects and is used extensively in this paper.

Some useful information can be obtained from a plot of log-slope versus defocus. As previously discussed, exposure latitude varies directly with the log-slope of the image. Thus, a minimum acceptable exposure latitude specification translates directly into a minimum acceptable value of the NLS. The log-slope versus defocus curve then can be used to give a maximum defocus to keep the process within this specification. If, for example, the minimum acceptable normalized log-slope of a given process was determined to be 3.5, the maximum defocus of 0.5- $\mu\text{m}$  lines and spaces on a 0.53 NA  $i$ -line stepper would be, from Fig. 2, about  $\pm 0.8 \mu\text{m}$ . This gives a practical definition of the depth of focus that separates the effects of the aerial image and the photoresist process. The printer determines the shape of the log-slope defocus curve, and the process determines the range of operation (i.e., the minimum NLS value). If the minimum log-slope needed was 6, one would conclude from Fig. 2 that this printer could not adequately resolve 0.5- $\mu\text{m}$  lines and spaces. Thus, resolution can also be determined from a log-slope defocus curve.

To define resolution consider Fig. 3, which shows the effect of feature size on the log-slope defocus curve. If, for example, a particular photoresist process requires an NLS of 3.8, one can see that the 0.4- $\mu\text{m}$  features will be resolved only when in perfect focus, the 0.5- $\mu\text{m}$  features will have a DOF of  $\pm 0.7 \mu\text{m}$ , and the 0.6- $\mu\text{m}$  features will have a DOF of  $\pm 0.9 \mu\text{m}$ . Obviously, the DOF is extremely sensitive to feature size, a fact that is not evident in the common Rayleigh definition. Because DOF is a strong function of feature size, it is logical that resolution is a function of the required DOF. Thus, in the situation shown in Fig. 3, if the minimum acceptable DOF is  $\pm 0.8 \mu\text{m}$  and the required NLS is 3.8, the practical resolution is about 0.55  $\mu\text{m}$  for equal lines and spaces. Resolution and depth of focus cannot be independently defined, but rather are interdependent. To summarize, depth of focus can be defined as the range of focus that keeps

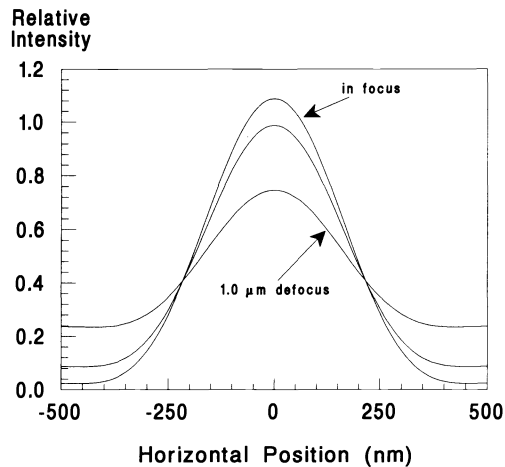


**Fig. 1** Effect of defocus on an aerial image (0.5- $\mu\text{m}$  lines and spaces;  $\text{NA} = 0.53$ ;  $i$ -line;  $\sigma = 0.5$ ; and defocus values of 0, 0.5, and 1.0  $\mu\text{m}$ ) simulated with PROLITH/2.

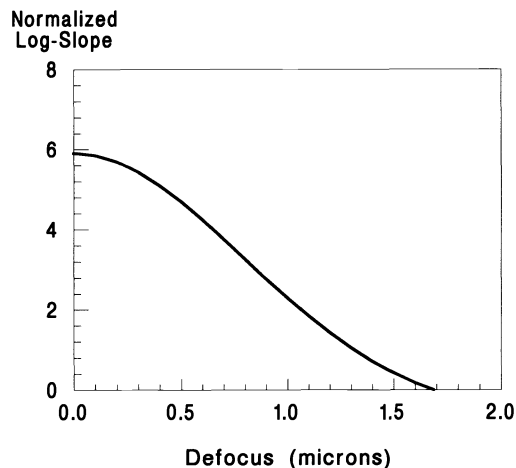


**Fig. 2** Example of the log-slope defocus curve (0.5- $\mu\text{m}$  lines and spaces,  $\text{NA} = 0.53$ ,  $i$ -line, and  $\sigma = 0.5$ ).

the log-slope above some specification for a given feature. Resolution can be defined as the smallest feature that keeps the log-slope above some specification over a given range of focus.

The key to these definitions for resolution and depth of focus is the linear correlation between the NLS and exposure latitude. But to make quantitative estimates, one must have a reasonable estimate for the minimum acceptable normalized log-slope. How is such an estimate obtained? By measuring a focus exposure matrix, one can obtain an experimental plot of exposure latitude versus defocus. This can be repeated for many different feature types and sizes, if desired. Figure 4(a) shows an example of such a plot where exposure latitude (EL) is defined as the range of exposure (as a percentage of the nominal dose) that keeps the linewidth within  $\pm 10\%$  of the nominal. Obviously, exposure latitude decreases greatly as the image is defocused. By comparing such experimental data with the log-slope defocus curves as in Fig. 3, a correlation between NLS and exposure latitude can be obtained.

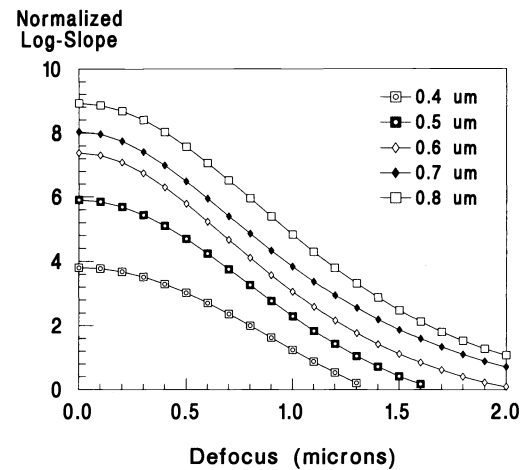


**Fig. 3** Log-slope defocus curves showing the effect of linewidth (equal lines and spaces,  $\text{NA} = 0.53$ ,  $i$ -line, and  $\sigma = 0.5$ ).

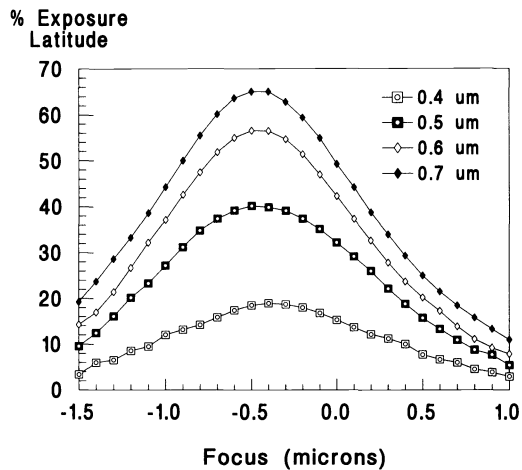
In this case, the data in Figs. 3 and 4(a) are correlated by the simple expression

$$\text{EL} = 8.1(\text{NLS} - 1.1) \quad (6)$$

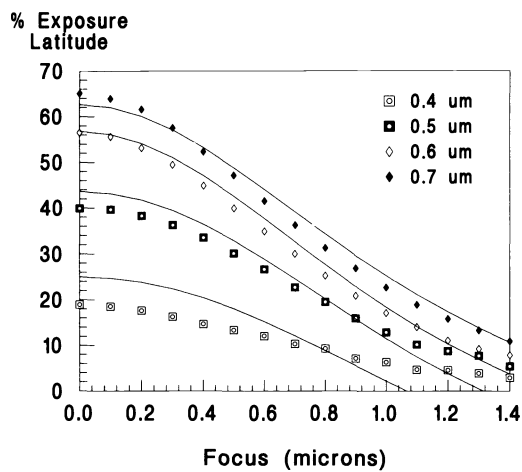
Figure 4(b) shows the goodness of the fit given by Eq. (6). Note that the smallest feature begins to deviate from this fit, indicating a nonlinear resist response below some feature size (this is directly analogous to the concept of the film MTF often used in the photographic sciences).

Equation (6) in and of itself leads to very revealing interpretations. First, note that an NLS of at least 1.1 must be used before an image in photoresist is obtained even at one exposure level. Above an NLS of 1.1, each increment in NLS adds 8.1% exposure latitude. Finally, if a minimum required exposure latitude is specified for a process, this value will translate directly into a minimum required NLS. For example, if an EL of 20% is required, the NLS that just achieves this level is 3.6. Thus, all images with a NLS in excess of 3.6 would be considered acceptable from an exposure latitude point of view. Correlations like Eq. (6) are very process dependent. However, for a given process, such a correlation allows imaging parameters to be studied by simply examining the log-slope defocus behavior.

The log-slope defocus curve can now be used to explore the effects of various parameters on the resolution and depth of focus. The numerical aperture is one of the most important parameters defining lithographic performance, and yet it is the most misunderstood. The Rayleigh DOF equation seems to predict a dramatic decrease in DOF with increasing numerical aperture. Shown in Fig. 5 is the effect of numerical aperture on the log-slope defocus curve of 0.5- $\mu\text{m}$  lines and spaces. The effect of increasing NA is to improve the aerial image log-slope when small amounts of defocus are present, and worsen the log-slope of an image with larger amounts of defocus. This is an extremely important result. Increasing the numerical aperture improves image quality only if focus errors can be kept below a certain value. In fact, for a given amount of defocus, there is an optimum NA that gives the largest log-slope. Similarly, for a given log-slope specification, there is one NA that maximizes the depth of focus.



(a)



(b)

**Fig. 4** Comparing exposure latitude with image log-slope: (a) simulated exposure latitude versus defocus for different line-widths and (b) comparison of the exposure latitude data (points) with the scaled NLS (lines) using  $\alpha=8.1$  and  $\beta=1.1$ . For (a), focus is defined relative to the top of the resist, with positive focus meaning focusing above the resist. In (b), best focus is set to zero for easier comparison with the log-slope curves.

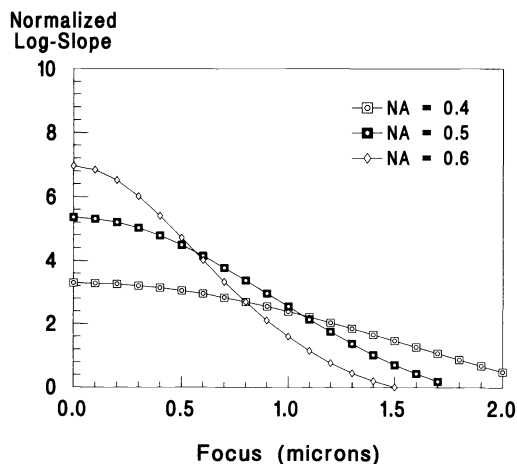


**Fig. 5** Effect of numerical aperture (NA) on the log-slope defocus curve (0.5- $\mu$ m lines and spaces, *i*-line, and  $\sigma=0.5$ ).

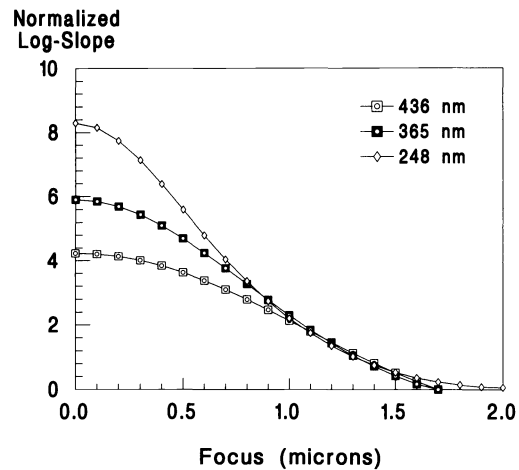


**Fig. 6** Effect of wavelength on the log-slope defocus curve (0.5- $\mu$ m lines and spaces, NA=0.53, and  $\sigma=0.5$ ).

The role of wavelength in depth of focus is also misunderstood. Although Eq. (2) seems to indicate worse DOF with shorter wavelength, Fig. 6 shows that DOF improves as wavelength decreases for a given feature size. Figures 5 and 6 show clearly the danger of using the Rayleigh criterion for comparing the DOF of different printers (i.e., different values of wavelength and numerical aperture).

The log-slope defocus curve can be used objectively to compare different printers. Recently there has been much discussion on the advantages of shorter wavelength versus higher numerical aperture. For example, one could compare an *i*-line, 0.53-NA system with a deep-UV 248-nm, 0.36-NA system. Both have the same value of  $\lambda/NA$  and thus, according to the Rayleigh criterion, the same resolution. In terms of the log-slope curve, the same value of  $\lambda/NA$  corresponds to the same value of the log-slope of the image with no defocus (Fig. 7). The practical resolution is defined as the smallest feature meeting a given log-slope specification over a given focus range. If a process requires a normalized log-slope of 3.5 and a focus budget of  $\pm 1 \mu\text{m}$ , Fig. 7 shows that the deep-UV system will resolve the 0.5- $\mu\text{m}$  feature, but the *i*-line system will not. Thus, the shorter wavelength system has better practical resolution than the *i*-line system even though  $\lambda/NA$  is the same for the two printers.

It is important to note that all of the aerial image calculations presented in this paper assume diffraction-limited lens performance, i.e., ideal lenses. Obviously, the ideal lens does not exist, and thus real lenses have log-slope versus defocus curves that are degraded to some extent from the ideal curves shown here. When comparing different lenses, as was done, one must keep in mind that one lens may be farther from the ideal than the other. Of course, if the amount of aberrations for a given lens is known, these aberrations can be included in the calculation of log-slope.

Other image-related parameters can be easily studied using the log-slope defocus curves. The differences between imaging dense and isolated features, or lines versus contacts, for example, can be examined. Partial coherence effects can be evaluated. The log-slope defocus approach has been used to optimize the numerical aperture and partial coherence of a stepper,<sup>9</sup> examine the differences between imaging in pos-

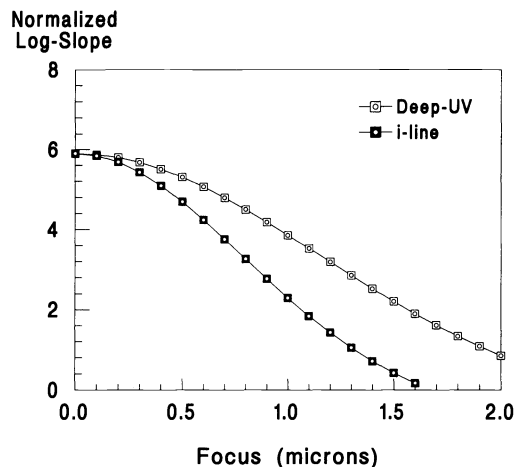


**Fig. 7** Comparison of two printers with the same value of  $\lambda/\text{NA}$  show that they have different practical resolutions (0.5- $\mu\text{m}$  lines and spaces,  $\sigma=0.5$ ; deep UV:  $\lambda=248$  nm,  $\text{NA}=0.36$ , i-line:  $\lambda=365$  nm, and  $\text{NA}=0.53$ ).

itive and negative tone resist,<sup>10</sup> and study the advantages of off-axis illumination.<sup>11</sup>

#### 4 Photoresist Effects

Although defocus is strictly an optical phenomenon, the photoresist plays a significant role in determining the effects of defocus. As one might imagine, a better photoresist provides greater depth of focus. In light of the preceding description of defocus using log-slope defocus curves, the photoresist impacts the DOF by changing the minimum acceptable log-slope specification. A better photoresist has a lower log-slope specification, resulting in a greater usable focus range. This relationship between the photoresist and the log-slope specification is determined experimentally as described above by measuring exposure latitude versus defocus. In general, the resulting correlation between the normalized log-slope (NLS) and the exposure latitude (EL) is given by

$$\text{EL} = \alpha(\text{NLS} - \beta) , \quad (7)$$

where  $\beta$  is the minimum NLS required to give any image at all in photoresist and  $\alpha$  is the percent increase in exposure latitude per unit increase in NLS. Thus, to a first degree, the effect of the photoresist on depth of focus can be characterized by the two parameters  $\alpha$  and  $\beta$ .

Consider for a moment an ideal, infinite contrast photoresist. For such a case, the slope of the exposure latitude curve will<sup>12</sup> be exactly  $2/\text{NLS}$  (see Appendix B for a derivation). Thus, using a typical linewidth specification of  $\pm 10\%$ , an infinite contrast resist would make  $\alpha = 10$  and  $\beta = 0$ . The quality of a photoresist with respect to focus and exposure latitude can be judged by how close  $\alpha$  and  $\beta$  are to these ideals.

Of course, the influence of the photoresist on focus effects is more complicated than the above first-order analysis would indicate. A second-order (but still very important) effect comes from the fact that the resist thickness is nonzero. Because the aerial image can be in focus at only one plane, at best only one location within the resist is in focus. This de-

focusing of the image as it propagates through the resist is important only when the thickness of the resist approaches the depth of focus. Historically, as the feature sizes of interest have decreased the DOF has been shrinking faster than the resist thickness. Thus, today's state-of-the-art lithography processes usually have resist thicknesses of the order of half of the resulting depth of focus.

The effect of a nonzero resist thickness is to cause an asymmetrical response to plus and minus focus. For the sake of this discussion, let us assume that best focus means placing the plane of best focus at the middle of the photoresist. By definition, we shall call a positive focal position focusing above the middle of the resist and a negative focal position shall mean focusing below this midpoint. Consider the effect of focusing below the resist (negative focus error). Obviously, the top of the photoresist will be more out of focus than the bottom. The result will be a photoresist profile (i.e., a cross-sectional view of a photoresist feature such as a line) that has a sharper, more ideal shape at the bottom than at the top, as seen in Fig. 8(a). By focusing above the resist, the bottom is farther out of focus than the top. In this case, the bottom will have a more rounded, out-of-focus shape to it than the top, as seen in Fig. 8(b). Figure 8 shows quite clearly that focusing above or below the optimum focus results in very different responses. Incidentally, best focus is often defined as that which gives the steepest sidewalls on a photoresist profile and usually occurs when focusing about in the middle of the photoresist.

The linewidth of a photoresist feature is one of those terms that in practice takes on many different definitions. One simple definition is the width of the photoresist profile at the resist/substrate interface. Definitions based on the top of the profile, the middle, or some average are also used. Because the shape of the photoresist profile is very different for positive defocus versus negative defocus, one would expect that the linewidth would also be different. As a result, Bossung curves, which plot linewidth versus focus for different exposures, are asymmetrical with respect to best focus. Figure 9(a) shows a typical set of Bossung curves and Fig. 9(b) shows the resulting process window. The process window is determined from the Bossung curves by plotting contours of constant linewidth over the range of focus and exposure. In particular, two contours, corresponding to the nominal linewidth  $\pm 10\%$ , are used to define a window. Values of focus and exposure that lie inside this window result in linewidths that are within the  $\pm 10\%$  specification. One can see that these curves are not symmetrical with respect to best focus. Further, because all linewidth measurement methods are, to some degree, dependent on resist profile, changing linewidth measurement methods can result in significant changes in the shape of the measured Bossung and process window curves.

#### 5 Methods of Depth-of-Focus Improvement

The term DOF is often used as a catchall for any focus effect in optical lithography. It is important to realize, however, that there are two distinct aspects of focus issues in manufacturing: process requirements and process capabilities. A particular process requires a minimum depth of focus because of numerous built-in focus errors of the process. For example, topography is a constant for a given layer and results in a direct focus error (the top and bottom of the topography cannot both be in focus). Built-in focus errors (BIFE) can be

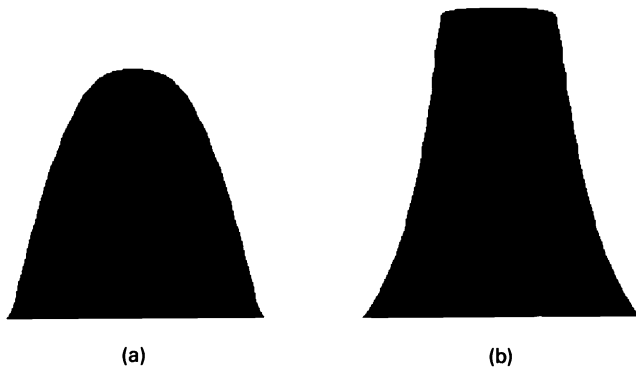


**Fig. 8** Photoresist profiles resulting from defocusing (a) below the resist and (b) above the resist. Profiles shown here are cross sections of long, isolated lines in positive photoresist.

**Table 1** Example of focus process requirement analysis.\*

Estimated Built In Focus Errors (BIFE)	Total Range ( $\mu\text{m}$ )
<b>Random Errors:</b>	
Lens Heating (compensated)	0.10
Environmental (compensated)	0.20
Mask Tilt ( $0.7 \mu\text{m} / 16$ )	0.05
Mask Flatness ( $2.0 \mu\text{m} / 16$ )	0.12
Wafer Flatness (25 mm field)	0.50
Chuck Flatness (25 mm field)	0.14
Autofocus Repeatability	0.20
Best Focus Determination	0.40
Vibration	0.10
<b>Total RSS Random Focus Errors:</b>	<b>0.74</b>
Topography	0.5
Field Curvature and Astigmatism	0.4
Resist Thickness	0.2
<b>Total BIFE (range)</b>	<b>1.8 <math>\mu\text{m}</math></b>

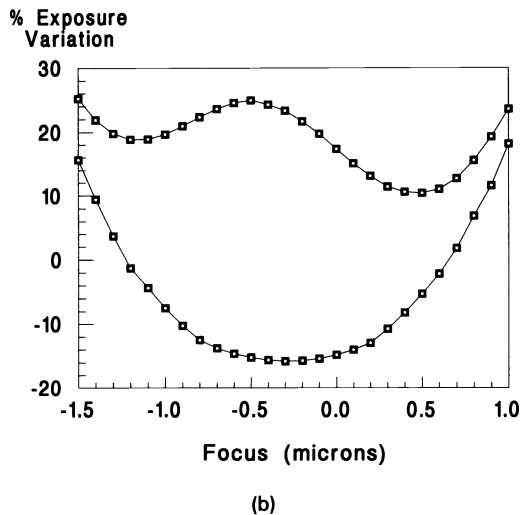
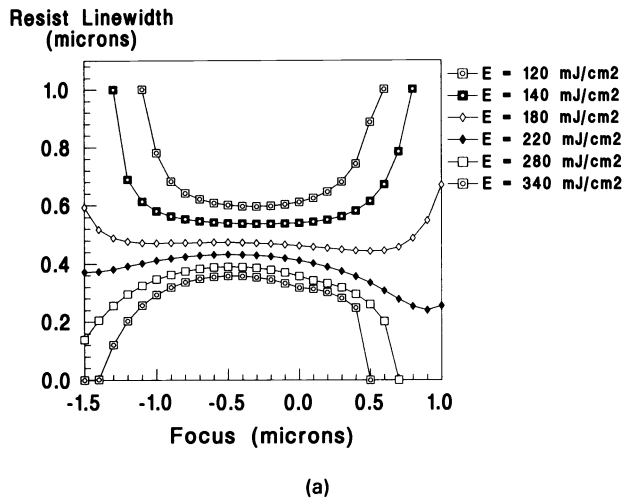


**Fig. 9** Focus exposure matrix linewidth data showing asymmetrical behavior plotted as (a) Bossung curves and (b) the  $\pm 10\%$  linewidth process window (0.5- $\mu\text{m}$  lines and spaces,  $\text{NA}=0.53$ ,  $f\text{-line}$ , and  $\sigma=0.5$ ).

either random (e.g., vibration) or systematical (e.g., topography). A careful analysis of the sources of BIFE is essential to determine a process focus requirement. Table 1 shows the results of a hypothetical analysis of a typical 0.5- $\mu\text{m}$  process with a  $4\times$  reduction stepper. Note that the random errors are first added rss (root sum square) and then added to the systematical errors. It is apparent from such an analysis which errors cause the greatest problems (in this case wafer non-flatness, best focus determination, topography, and field curvature and astigmatism).

Independent of process requirements, process capability describes how a lithographic process responds to focus errors. Depth of focus is actually a term that describes process capability, but it is so often misused that it can mean virtually anything depending on the context. A less-abused term is focus latitude, which can be defined as the response of the process to a given error in focus. If the process capability exceeds the process requirements, then reasonable manufacturing yields can be obtained. Because the ultimate goal is yield, the lithographer can either reduce the process requirements (by reducing the BIFE) or increase the process capability (by increasing the DOF) to achieve improved yield. Any successful strategy for scaling a process to smaller dimensions must encompass both of these approaches.

Defining focus latitude is complicated by its extreme dependence on exposure energy, just as exposure latitude is dependent on focus. Thus, a definition of DOF is only useful if it describes the coupled exposure-focus dependency. The best description of DOF comes from the focus-exposure process window, which was described briefly in the previous section. For a given process specification, the focus-exposure process window is a plot of all those values of focus and exposure that keep the process within specification. The most common specifications are linewidth and resist sidewall angle, but resist loss can also be used. It is important to note that the measurement process may introduce focus errors (autofocus repeatability, wafer nonflatness) and thus the measured focus latitude may in fact be a resultant latitude after several errors have been introduced. Usually it is best to try to minimize these errors when measuring focus latitude (use ultraflat wafers, use only one field position, perform the experiment over a short period of time to eliminate environmental drift, etc.).

The following sections describe a variety of techniques that have been proposed to improve the depth of focus for high-resolution lithography processes. Some techniques are quite old (properly biasing the mask), but still have not found widespread use. Some techniques are old to optics but new to lithography (spatial filtering, phase-shifting masks) and still unproven. The goal here is to give some indication of the benefits and detriments of each method.

### 5.1 Mask Bias

Originally, adding bias to a mask was used as a means of compensating for subsequent process steps that changed the dimensions of the final structure from that defined in the lithographic step. With the advent of high-resolution positive resists, it became known that process latitude could be improved by overexposing. Thus, by oversizing the chrome features on the mask and overexposing the resist, correct linewidths could be obtained with improved latitude. The drawback, of course, was throughput. There are two main reasons why this type of biasing works: (1) improvement of the latent image through higher exposures<sup>5</sup> and (2) improvement of the image log-slope.<sup>13</sup>

The simplest way to bias a mask is to apply the same bias to all features. However, not all features need the same bias. In fact, the simplicity of a uniform bias is the main reason why bias is not used to its full potential. For each feature, there is an optimum bias that maximizes the size of its process window. Further, the optimum bias varies considerably with feature size and type.<sup>13</sup> For example, isolated lines benefit greatly from a relatively large amount of bias, but high-resolution line/space arrays do not. What is needed is a geometry-dependent bias. Implemented as a computer-aided design (CAD) algorithm, geometry dependent bias would examine the feature size and type and the proximity of other features to determine the amount of bias based on the following two criterion. First, the critical feature(s) would be biased to improve performance. Next, the rest of the mask would be biased to print properly at the energy needed to print the critical feature(s). Although significantly more complicated than a uniform bias, an algorithm of this type is certainly within our capabilities. Yet, only recently have attempts to define such an algorithm for limited structures been published.<sup>14</sup> It is interesting to note that such an algorithm is a subset of the problem that must be solved to design optimized phase-shifting masks. Thus, industry focus on the problem of geometry-dependent bias would find immediate benefit and serve as an important first step in the automated design of phase-shifting masks.

### 5.2 Variable Numerical Aperture and Partial Coherence

In 1989 the author introduced the concept of "image manipulation," varying the numerical aperture (NA) and partial coherence  $\sigma$  of a stepper on a level-by-level basis to optimize the shape of the aerial image for the critical feature(s) on each mask level.<sup>9,15</sup> The effect of numerical aperture on DOF is not obvious and is strongly dependent on the feature size and type as well as the partial coherence. As was discussed earlier, for a given amount of defocus there is one value of the numerical aperture that gives the maximum log-slope of the aerial image. This optimum NA is also a function of

feature type and size and is strongly dependent on the partial coherence. For a given feature type and size and a given amount of defocus, there is one value of NA and  $\sigma$  that gives optimum image quality. Likewise, for a given feature type and size and a minimum acceptable image quality (i.e., minimum value of the normalized log-slope) there is one NA and  $\sigma$  that gives the maximum DOF.

Consider the imaging of 0.45- $\mu\text{m}$  lines and spaces with conventional *i*-line illumination assuming 0.75  $\mu\text{m}$  of defocus is expected in the process (i.e., one half of the BIFE). By varying both the numerical aperture and the partial coherence, contour plots of constant image log-slope can be generated, as shown in Fig. 10. In this case, the optimum log-slope occurs when NA = 0.45 and  $\sigma = 0.10$  (where a value of 0.1 was the lowest examined). If one were to repeat this analysis for 0.4- $\mu\text{m}$  lines and spaces, however, the optimum NA would be 0.55 with  $\sigma = 0.65$ , indicating extreme feature size sensitivity to the optimum values.

Although a very useful indicator, it is not possible to determine the true optimum values of NA and  $\sigma$  based solely on log-slope. Another approach is to use the lumped parameter model (LPM) to predict the size of the process window.<sup>12</sup> The LPM is a simple model for resist exposure and development that allows for the calculation of an entire focus-exposure matrix on a PC in a matter of seconds. Although certainly not as accurate as the primary parameter models found in programs such as PROLITH/2 and SAMPLE, the LPM is more accurate than any metric based solely on aerial images (e.g., the image log-slope). Using an optimization routine built into PROLITH/2, numerical aperture and partial coherence can be varied to maximize the size of the focus-exposure process window (as predicted by the LPM over a specified focus range). Based on this approach, the discussed case of 0.45- $\mu\text{m}$  lines and spaces has an optimum LPM process window, when NA = 0.49 and  $\sigma = 0.22$ , versus the NA = 0.45 and  $\sigma = 0.1$  given by the maximum log-slope method. Both the log-slope and LPM approaches can be used to quickly determine the approximate optimum stepper settings, which can then be investigated further with the more exact primary parameter models and finally experimental data.

### 5.3 Multiple-Focal-Plane Exposures

Recently, Fukuda and coworkers<sup>16-18</sup> from Hitachi introduced a method, which they called FLEX, with the potential to improve depth of focus. In its simplest form, a wafer would be given a partial exposure at a particular focal position. Then, without moving the wafer in the *x* or *y* directions, the wafer would be moved to a different focal position and the remaining exposure would be delivered. The result is an averaging of aerial images both in and out of focus. Although two focal plane exposures are a minimum, more focal planes can be used. Typically, only two or three planes have been used because more exposures tend to add complexity without giving further benefit. In addition to processing complexity and decreased throughput, what are the trade-offs of using this technique? How much benefit can be expected?

The log-slope defocus curve again is a useful technique for understanding the effects on DOF. For a multiple focal plane exposure, the final aerial image can be thought of as a summation of the aerial images at the different focal planes, weighted by their respective exposure energies. For the cases

**Numerical Aperture**

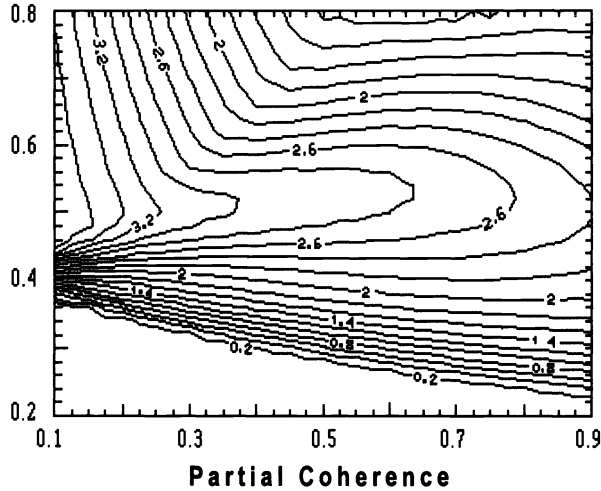
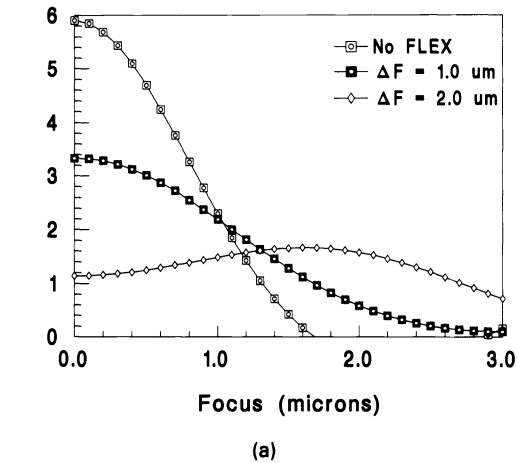


**Fig. 10** Contour map of image log-slope as a function of the numerical aperture and partial coherence of the projection system (0.45- $\mu\text{m}$  lines and spaces,  $i$ -line, and 0.75- $\mu\text{m}$  defocus).

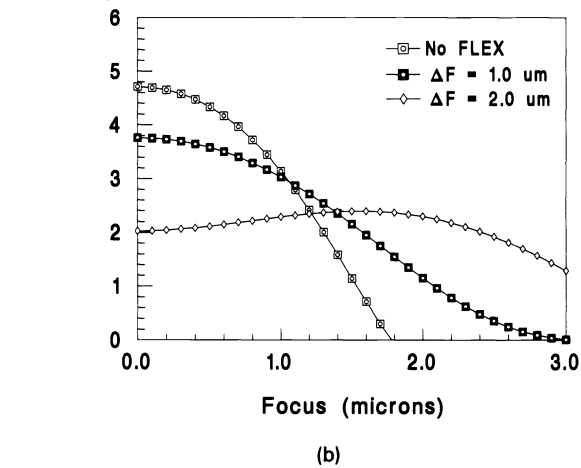
studied here, three focal planes are used separated from each other by a distance  $\Delta F$ , all with equal exposures. Once an average aerial image is computed, its log-slope can also be determined. Figure 11(a) shows the effect of  $\Delta F$  on the log-slope defocus response for 0.5- $\mu\text{m}$  lines and spaces (NA = 0.53,  $\sigma = 0.5$ , and  $i$ -line). A  $\Delta F = 0$  indicates the standard single-focal-plane exposure. Some statements can be made about this graph that I have found to be generally true for multiple focal plane exposures: (1) this technique results in improved log-slope for out-of-focus conditions, but only at the expense of reduced performance in focus, and (2) the focus value at which the curves cross (in this case both are at about 1.2  $\mu\text{m}$  of defocus) is beyond what would normally be considered the depth of focus of the system. Further, for the case of equal lines and spaces, the crossover point occurs at an extremely low value of log-slope, making the use of FLEX for lines and spaces undesirable.

Figure 11(b) shows the same simulations for the case of an array of 0.5- $\mu\text{m}$  contacts. The basic trends are the same, but now the crossover point occurs at a much more reasonable, although still low, value of the normalized log-slope. Although the log-slope defocus curve gives a great deal of insight into the behavior of multiple-focal-plane exposures, it does not tell the full story. In particular, the log-slope defocus curve gives no information about isofocal bias. The isofocal bias is the difference between the linewidth that has the least sensitivity to focus and the nominal linewidth. For example, the Bossung curves in Fig. 9(a) show a slight isofocal bias with the flattest curves occurring at a linewidth of about 0.45  $\mu\text{m}$  for a nominal linewidth of 0.5- $\mu\text{m}$  features. The process window of Fig. 9(b) also indicates an isofocal bias by the upward curvature of the window. Considering again the contacts, Fig. 12(a) shows a focus-exposure process window for a 0.5- $\mu\text{m}$  contact with a standard single-pass exposure. Values of focus and exposure that are within this window have linewidths within  $\pm 10\%$  of the nominal value. A limiting feature of this window is its curvature. As the contact goes out of focus, more energy is required to properly

**Normalized Log-Slope**



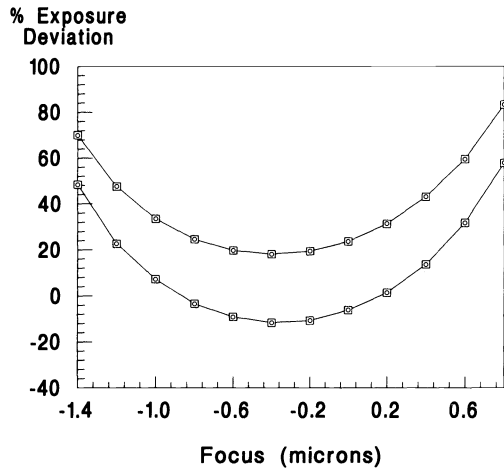
**Normalized Log-Slope**



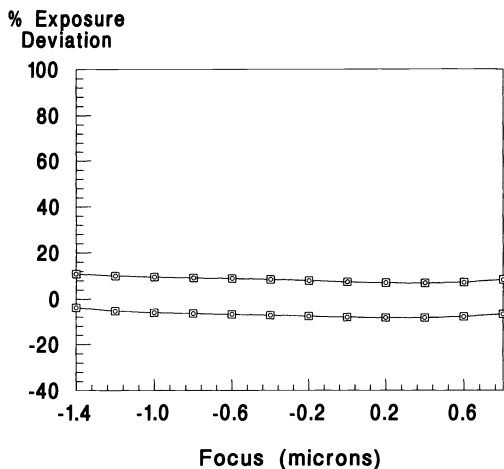
**Fig. 11** Log-slope defocus curves showing the effect of aerial image averaging through focus using a three-pass, multiple-focal-plane exposure with a focal plane separation of  $\Delta F$  for (a) 0.5- $\mu\text{m}$  equal lines and spaces and (b) 0.5- $\mu\text{m}$  contacts.

size it. Thus, the curvature of the window is indicative of an extreme isofocal bias, which will significantly limit the overall depth of focus. The log-slope defocus curve gives no indication that this isofocal bias exists. Examining the process window resulting from a three-pass, multiple-focal-plane exposure with  $\Delta F = 1.5 \mu\text{m}$  [Fig. 12(b)], one can see that the isofocal bias has essentially been eliminated. Although the size of the window in focus has diminished (i.e., there is less exposure latitude in focus), the window stays essentially the same size over a long focus range. Thus, if the smaller exposure latitude is acceptable, the DOF of these contacts can be improved using FLEX.

Figure 12 shows that the main benefit of the FLEX method for contacts is to reduce, or even eliminate, the isofocal bias. In fact, the optimum focal plane separation can be found as the value that completely eliminates the isofocal bias (in this case, this value is slightly greater than 1.5  $\mu\text{m}$ ). The price that must be paid is a reduction in exposure latitude and



(a)



(b)

**Fig. 12** Effect of multiple-focal-plane exposures on the shape of the focus-exposure process window of 0.5- $\mu\text{m}$  contacts: (a) no FLEX and (b) three-pass exposure using  $\Delta F = 1.5 \mu\text{m}$ .

photoresist sidewall angle when in focus. The unique imaging attributes of contacts in positive photoresist (i.e., a strong isofocal bias) make the FLEX method particularly appropriate, whereas other types of features do not show much potential for benefit.

#### 5.4 Spatial Frequency Filtering

The concept of spatial frequency filtering is not a new one. The earliest filter to be studied was the simple annular aperture in which the central portion of the objective lens pupil is blocked. The use of an annular aperture was first suggested by Lord Rayleigh<sup>19</sup> as a means of improving resolution, although it had been studied mathematically much earlier. Steward<sup>20</sup> studied this aperture and found that it gave “a decided gain in resolving power” at the expense of throughput due to the loss of light. Welford<sup>21</sup> later studied annular apertures and found that they also improved depth of focus, but produced secondary image maxima of greater intensity (commonly called side-lobes today). Welford also suggested

that proper adjustment of the response of the photographic media could reduce the printability of these sidelobes, as has been recently suggested for photoresists.<sup>22</sup> Jacquot et al.<sup>23</sup> described an application in which the outer portions of the aperture were reduced in transmission and coined the term apodization to describe this filtering technique. Although the result of this filter is reduced resolution, the use of the term apodization has grown to encompass any modification of the transmission properties, real or complex, of a lens pupil (for an early review of work in this area, see Ref. 24). Duffieux is given credit for introducing Fourier frequency analysis to optics in his 1946 book, which has only recently been translated into English.<sup>25</sup> Thus, modification of the transmission function of a lens aperture has come to be known as spatial frequency filtering (see Goodman’s<sup>26</sup> classic textbook for a review of spatial filtering). In fact, the effect of a central aperture stop on the frequency response of an imaging system is given as a homework problem by Goodman (Ref. 26, Chap. 6, problem 6-1).

Recently, spatial filtering has been proposed for microlithography.<sup>27,28</sup> The proposed filters have been similar in principle to an annular aperture, but rather than having a transmission of zero in the central portion of the aperture the transmission is simply reduced. For example, a filter may have a transmission of 50% out to a radius of one half of the pupil radius, with 100% transmission for the outer half of the pupil. Although a pure transmission filter would be much simpler to fabricate, shifters could be added as well. Thus, for example, our simple filter could be modified to have 50% transmission and a 180-deg phase shift in the central portion of the aperture. In general, a radially symmetrical filter can be described by its complex transmission function  $\tau(\rho)$ , where  $\rho$  is the radial position within the pupil relative to the pupil diameter.

As an example of the effect of a simple filter on a simple aerial image, consider the coherent image of a 0.5- $\mu\text{m}$  line/space array such that only the zero and first diffraction orders make it through the lens. The resulting aerial image intensity is given by

$$I(x) = \left[ \frac{1}{2} + \frac{2}{\pi} \cos(2\pi x/p) \right]^2, \quad (8)$$

where the cosine term results from the first diffraction orders and the one-half term results from the zero order. Consider now our simple filter where the central portion of light in the aperture is attenuated by passing through a filter with electric field transmission  $T$ . Further, let us pick the radius of this central region to be such that the zero order is attenuated but the first order is not. Thus, the filtered aerial image is

$$I(x) = \left[ \frac{1}{2} T + \frac{2}{\pi} \cos(2\pi x/p) \right]^2. \quad (9)$$

It is a simple matter to plot Eq. (9) and determine the effect of various transmissions on the image, as shown in Fig. 13, where each image was normalized to have the same peak intensity for comparison purposes. The effects are as expected. The edge slope of the space increases as the transmission is reduced, but at the expense of increased sidelobe intensity. In fact, if  $T = 0$ , the result is a dark-field frequency-doubled image.

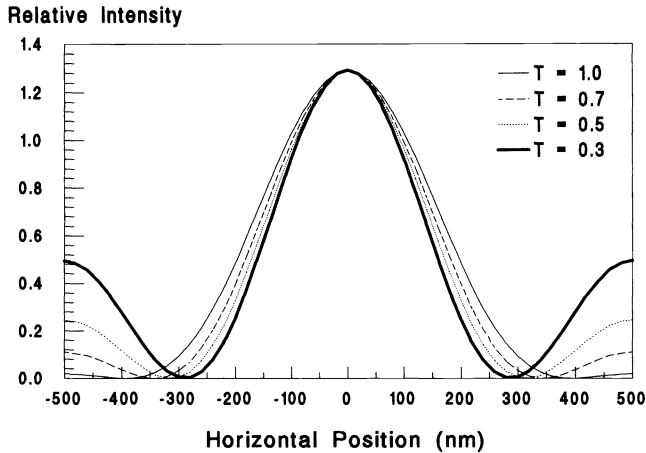


**Fig. 13** Effect of spatial filtering on an image of equal lines and spaces with coherent illumination for a simple filter that reduces the amplitude of the zero order by  $T$ . Images are normalized to have the same peak intensity for comparison purposes.

Of course, more complicated filters will have different responses, but the general trends will be similar. Several notes of caution are in order. For any given filter, the effect on the aerial image will be different for different feature sizes and types. Thus, in general, the first casualties of spatial frequency filtering are mask linearity and the proximity effect. These issues must be looked at very closely when designing a filter. A filter design can be fully optimized only for a particular feature. Thus, to get the most out of such a filter arrangement the filters must be easily interchangeable so that different mask levels can each be optimized. In light of these issues, it would be highly desirable to have only one critical feature per mask level when using spatial filtering.

### 5.5 Annular and Other Illumination Sources

Variations of the method of illumination seem to have received very little attention over the years as a means of improving imaging. Recently, both theoretical<sup>11,15</sup> and experimental<sup>29</sup> studies have shown the potential for improving image quality with annular illumination systems. Very recently, the use of various illumination shapes has generated considerable interest.<sup>30-32</sup>

The effect of annular illumination can be summed up quite nicely by examining the variation of the aerial image log-slope with linewidth. Figure 14 compares this variation for both conventional and annular illumination systems. As can be seen, the annular source results in improved image quality for certain small features (in this case for features near 0.3  $\mu\text{m}$ ) at the expense of reduced image quality for larger features (0.4 to 0.7  $\mu\text{m}$  here). This is the essential trade-off for any illumination modification. If the response of one feature size is improved, other features suffer. Thus, as before, there is an advantage to using various illuminator shapes, but only if they are easily changeable and if there are very few (preferably one) critical features per mask level.

### 5.6 Phase-Shifting Masks

The invention of phase-shifting masks for photolithography is generally attributed to Levenson et al.,<sup>6</sup> although mention of the technique is buried in the claims of a patent on x-ray

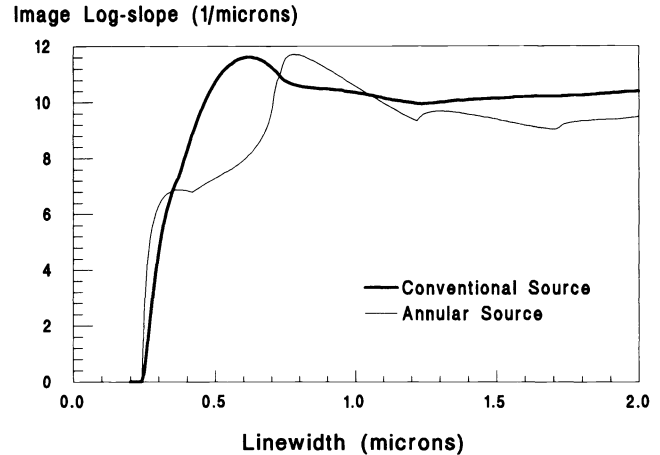


**Fig. 14** Comparison of conventional and annular sources for line/space pairs of varying width ( $\text{NA}=0.5$ ,  $i$ -line, no defocus,  $\sigma=0.5$  for the conventional source, and the annular source is a very thin annulus about  $\sigma=0.5$ ).

lithography.<sup>33</sup> In fact, the use of phase information on the object to improve resolution has been well known in optics for some time (see Ref. 26, p. 131). The so-called Levenson technique (also called the alternating aperture method) employs phase shifts of 0 and 180 deg in alternating apertures of a periodic structure (e.g., equal lines and spaces). The result is a decrease in the smallest printable feature size by up to a factor of 2. This dramatic improvement in resolution is seen as a method of extending the useful life of optical lithography by one to two generations. Interest in phase-shifting masks (PSMs) has increased greatly in the past 3 years as several companies have demonstrated<sup>34,35</sup> the fabrication of prototype circuits using PSMs.

As work proceeds, people are discovering that the use of phase information on the mask can greatly complicate the design of the mask, as well as our understanding of the imaging process. Rather than attempt to address all of the many issues involved in PSM lithography, this section simply describes one important type of PSM, the isolated phase edge, that is, an instantaneous transition from 0 to 180 deg phase removed from any other features on the mask. Such transitions can occur in chromeless, alternating aperture, rim shifter, and subresolution type PSM methods. It is well known that a 180-deg phase transition results in a dark line in the aerial image. In fact, phase edges have been used to print very high resolution lines in positive photoresist.<sup>36</sup> Some interesting questions arise as to the lithographic properties of such lines. Because the mask contains no information as to the width of these lines, what determines linewidth for a phase-edge mask? What is the quality of the aerial image (i.e., what is its log-slope)? These questions can be answered by a straightforward analysis of the imaging of phase edges.

The diffraction pattern for a perfect phase-edge mask feature can be obtained from the Fourier transform of the mask pattern.

$$M(f_x) = \frac{i}{\pi f_x}, \quad (10)$$

where  $f_x$  is the spatial frequency. Using this diffraction pat-

tern, the aerial image for coherent illumination can be obtained<sup>37</sup>:

$$I(x) = \frac{4}{\pi^2} Si^2\left(\frac{2\pi NAx}{\lambda}\right), \quad (11)$$

where

$$Si(\theta) = \int_0^\theta \frac{\sin z}{z} dz.$$

Figure 15 shows the resulting aerial image.

What will be the width of a line printed with the aerial image of Eq. (11)? Typically, the nominal width of a feature occurs where the aerial image intensity is in the range of 0.25 to 0.3 relative to the intensity in a large clear area. The “width” of the aerial image of a phase edge can thus be estimated by the 0.25 intensity contour line and, from Eq. (11), corresponds to a width of about

$$w = 0.25 \frac{\lambda}{NA}. \quad (12)$$

Thus, the width of a feature printed using a phase edge is determined by the wavelength and the numerical aperture. Note that the feature size defined by Eq. (12) is a factor of 2 less than what is generally considered to be the resolution limit of an imaging system. This value of the linewidth can be thought of as the natural linewidth of a 0- to 180-deg phase transition. Further, by properly adjusting the partial coherence, this very small feature can be printed over a reasonable range of focus.<sup>37</sup>

In general, proper use of phase-shifting masks can improve the depth of focus for very small features. However, as with many of the image enhancing techniques, proximity effects and mask linearity often suffer. In addition, the design and fabrication of PSMs present many formidable technical hurdles that will not be easily overcome.

## 6 Conclusions

The Rayleigh criteria for resolution and depth of focus are not adequate in describing submicrometer optical lithography. In fact, it is quite easy to misinterpret the Rayleigh criteria and draw completely inaccurate conclusions. Thus, a more rigorous approach to characterizing resolution and depth of focus is required. By examining the interaction of the lithographic tool (via the aerial image) with the photoresist process, a metric for judging aerial image quality has been established—the image log-slope. By examining the effects of this metric on feature size and defocus, accurate and meaningful definitions of resolution and depth of focus can be made. This technique also leads to an understanding of the influence of various parameters on the depth of focus/resolution and the ability to compare the theoretical performance of different lithographic tools.

Photoresist was shown to have a major impact on the response of the process to changes in focus. First, improving the photoresist results in improved exposure latitude. This in turn allows the image to be further degraded by focus errors and still give acceptable results. Second, submicrometer op-

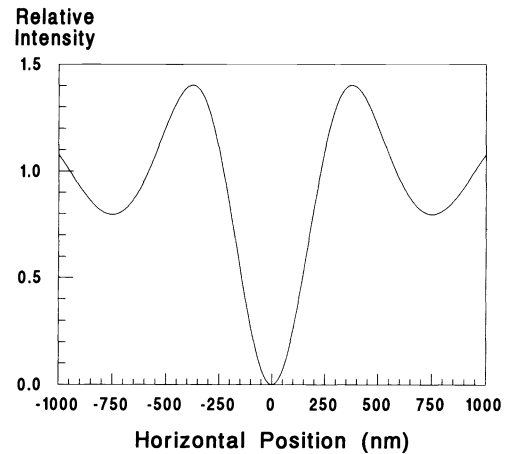


**Fig. 15** Aerial image for an isolated 0- to 180-deg phase edge under coherent illumination ( $\lambda = 365$  nm and  $NA = 0.5$ ).

tical lithography usually results in asymmetrical focus behavior because of the defocusing of the aerial image as it propagates through the photoresist. Finally, several methods for depth-of-focus improvement were reviewed. All gave some improvement in depth of focus under certain conditions, but none proved to be a panacea. Of course, one important alternative is to work to reduce the magnitude of built-in focus errors.

## 7 Appendix A

The use of contrast to describe the response of a photosensitive material dates back over 100 years. Hurter and Driffield<sup>38</sup> measured the optical density of photographic negative plates as a function of exposure. The “perfect” negative was one that exhibited a linear variation of optical density with the logarithm of exposure and a plot of optical density versus log-exposure showed that a good negative exhibited a wide “period of correct representation.” Hurter and Driffield (H-D) called the slope of this curve in the linear region  $\gamma$ , the “development constant.” Negatives with high values of  $\gamma$  were said to be “high-contrast” negatives because the photosensitive emulsion quickly changed from low to high optical density when exposed. Of course, high-contrast film is not always desirable because it easily saturates.

Photolithography evolved from photographic science and borrowed many of its concepts and terminology. When exposing a photographic plate, the goal is to change the optical density of the material. In lithography, the goal is to change the development rate of the photoresist. Thus, the analogous H-D curve for lithography plots log-development rate versus log-exposure. Following the definition of  $\gamma$  from Hurter and Driffield, the photoresist contrast can be defined as

$$\gamma \equiv \frac{\partial \ln R}{\partial \ln E}, \quad (13)$$

where  $R$  is the resist development rate and  $E$  is the exposure energy. Note that this definition of contrast has been called the theoretical contrast by the author<sup>5,39</sup> to distinguish it from the often misquoted measured contrast based on the photoresist contrast curve of resist thickness remaining versus log-exposure dose.

The goal of lithographic exposure is to turn a gradient in exposure energy (an aerial image) into a gradient in development rate. Because intensity  $I$  and energy are related by a constant (the exposure time),  $\partial \ln E = \partial \ln I$ . Thus, from Eq. (13), it is very easy to express the development rate gradient as<sup>5,39</sup>

$$\frac{\partial \ln R}{\partial x} = \gamma \frac{\partial \ln I}{\partial x}, \quad (14)$$

where  $x$  is the horizontal distance from the center of the feature being printed. The left-hand term is the spatial gradient of development rate. To differentiate between exposed and unexposed areas, it is desirable to have this gradient as large as possible. The right-hand side of Eq. (14) contains the log-slope of the aerial image. This term represents the quality of the aerial image, or alternatively the amount of information contained in the image about the position of the mask edge. The photoresist contrast amplifies the information content of the image and transfers it into the photoresist as a development rate gradient. This expression quite clearly illustrates the role of contrast in defining the goodness of a photoresist process.

## 8 Appendix B

The relationship between the normalized log-slope (NLS) of the aerial image and exposure latitude has been discussed before<sup>12</sup> and is briefly reviewed here. Consider, in the limiting case, an ideal threshold photoresist, one that has a high development rate for exposure energies above some  $E_{th}$  and zero development rate for energies below this value. For such a case, the linewidth  $w$  formed on exposure to some aerial image  $I(x)$  is determined by the nominal exposure dose  $E$  and the spatial intensity variation of the image. That is,

$$EI(w/2) = E_{th}. \quad (15)$$

To determine how linewidth varies with exposure dose, one simply has to take the derivative of this equation.

$$2 \frac{\partial \ln E}{\partial w} = - \frac{\partial \ln I}{\partial x}. \quad (16)$$

Ignoring the sign and normalizing by multiplying both sides of the equation by the linewidth,

$$2 \frac{\partial \ln E}{\partial \ln w} = \text{NLS}. \quad (17)$$

Equation (17) tells us that, for an ideal threshold photoresist, the slope of an exposure latitude curve (log-linewidth versus log-exposure dose) will be  $2/\text{NLS}$ . We can interpret  $\partial \ln E$  as a percentage change in exposure and  $\partial \ln w$  as the resulting percentage change in linewidth. Assuming a typical linewidth specification for  $\partial \ln w$  would allow the term  $\partial \ln E$  to be interpreted as the exposure latitude (EL), the percentage change in exposure that keeps the linewidth within specification. Letting this linewidth specification be  $\pm 10\%$  (for a total range of 20%), the ideal exposure latitude would be given by

$$\text{EL} = 10 \text{ NLS}. \quad (18)$$

A real (nonideal) photoresist would have an exposure latitude less than this amount.

## References

1. C. A. Mack, "Understanding focus effects in submicron optical lithography," in *Optical/Laser Microlithography, Proc. SPIE 922*, 135–148 (1988); and *Opt. Eng.* **27**(12), 1093–1100 (1988).
2. C. A. Mack, "Comments on 'Understanding focus effects in submicrometer optical lithography,'" *Opt. Eng.* **29**(3), 252 (1990).
3. C. A. Mack and P. M. Kaufman, "Understanding focus effects in submicron optical lithography, part 2: photoresist effects," in *Optical/Laser Microlithography II, Proc. SPIE 1088*, 304–323 (1989).
4. C. A. Mack, "Understanding focus effects in submicron optical lithography, part 3: methods for depth-of-focus improvement," in *Optical/Laser Microlithography V, Proc. SPIE 1674*, 272–284 (1992).
5. C. A. Mack, "Photoresist process optimization," presented at KTI Microelectronics Seminar Interface '87 (1987).
6. M. D. Levenson, D. S. Goodman, S. Lindsey, P. W. Bayer, and H. A. E. Santini, "The phase-shifting mask II: imaging simulations and submicrometer resist exposures," *IEEE Trans. Electron Devices* **ED-31**(6), 753–763 (1984).
7. H. J. Levinson and W. H. Arnold, "Focus: the critical parameter for submicron lithography," *J. Vac. Sci. Tech.* **B5**(1), 293–298 (1987).
8. W. H. Arnold and H. J. Levinson, "Focus: the critical parameter for submicron optical lithography: part 2," in *Optical Microlithography VI, Proc. SPIE 772*, 21–34 (1987).
9. C. A. Mack, "Algorithm for optimizing stepper performance through image manipulation," in *Optical/Laser Microlithography III, Proc. SPIE 1264*, 71–82 (1990).
10. C. A. Mack and J. E. Connors, "Fundamental differences between positive and negative tone imaging," in *Optical/Laser Microlithography V, Proc. SPIE 1674*, 328–338 (1992); and *Microlithogr. World* **1**(3), 17–22 (1992).
11. C. A. Mack, "Optimization of the Spatial Properties of Illumination," in *Optical/Laser Microlithography VI, Proc. SPIE 1927* (in press, 1993).
12. C. A. Mack, A. Stephanakis, and R. Hershel, "Lumped parameter model of the photolithographic process," in *Proc. Kodak Microelectronics Seminar*, pp. 228–238 (1986).
13. C. A. Mack and P. M. Kaufman, "Mask bias in submicron optical lithography," *J. Vac. Sci. Tech.* **B6**(6), 2213–2220 (1988).
14. N. Shamma, F. Sporon-Fieller, and E. Lin, "A method for correction of proximity effect in optical projection lithography," *Proc. KTI Microelectronics Seminar*, pp. 145–156 (1991).
15. C. A. Mack, "Optimum stepper performance through image manipulation," in *Proc. KTI Microelectronics Seminar*, pp. 209–215 (1989).
16. H. Fukuda, N. Hasegawa, T. Tanaka, and T. Hayashida, "A new method for enhancing focus latitude in optical lithography: FLEX," *IEEE Electron Devices Lett.* **EDL-8**(4), 179–180 (1987).
17. T. Hayashida, H. Fukuda, T. Tanaka, and N. Hasegawa, "A novel method for improving the defocus tolerance in step and repeat photolithography," in *Optical Microlithography VI, Proc. SPIE 772*, 66–71 (1987).
18. H. Fukuda, N. Hasegawa, T. Toshihiko, and T. Kurosaki, "Method for forming pattern and projection aligner for carrying out same," U.S. Patent No. 4,869,999 (Sep. 1989).
19. Lord Rayleigh, "On the diffraction of object glasses," *Astronom. Soc. Monthly Notice*, **33**, 59–63 (1872); also reprinted in his book *Scientific Papers Vol. I*, pp. 163–166, Dover Publications, New York (1964).
20. G. C. Steward, *The Symmetrical Optical System*, pp. 88–94, Cambridge University Press, London (1928).
21. W. T. Welford, "Use of annular apertures to increase focal depth," in *J. Opt. Soc. Am.* **50**(8), 749–753 (1960).
22. P. M. Spragg, G. T. Dao, S. G. Hansen, R. F. Leonard, M. A. Toukhy, R. Singh, and K. K. H. Toh, "Optimization of positive novolak-based resists for phase shift mask technology," in *Optical/Laser Microlithography V, Proc. SPIE 1674* (1992).
23. P. Boughon, B. Dossier, and P. Jacquinet, *C. R. Acad. Sci.* **223**, 661 (1946) (in French).
24. E. Wolf, "The diffraction theory of aberrations," *Rep. Prog. Phys.* **14**, 109–111 (1951).
25. P. M. Duffieux, *The Fourier Transform and Its Application to Optics*, John Wiley & Sons, New York (1983).
26. J. W. Goodman, *Introduction to Fourier Optics*, McGraw-Hill, New York (1968).
27. H. Fukuda, T. Terasawa, and S. Okazaki, "Spatial filtering for depth-of-focus and resolution enhancement in optical lithography," *J. Vac. Sci. Technol.* **B9**(6), 3113–3116 (1991).
28. W. Henke and U. Glaubitz, "Increasing resolution and depth-of-focus in optical microlithography through spatial filtering techniques," in *Microcircuit Engineering '91*, Elsevier Science Pub., Amsterdam (1991).

29. D. L. Fehrs, H. B. Lovering, and R. T. Scruton, "Illuminator modification of an optical aligner," in *Proc. KTI Microelectronics Seminar*, pp. 216–230 (1989).
30. M. Noguchi, M. Muraki, Y. Iwasaki, and A. Suzuki, "Subhalf micron lithography system with phase-shifting effect," in *Optical/Laser Microlithography V, Proc. SPIE 1674*, 92–104 (1992).
31. N. Shiraishi, S. Hirukawa, Y. Takeuchi, and N. Magome, "New imaging technique for 64MDRAM," *Optical/Laser Microlithography V, Proc. SPIE 1674*, 741–752 (1992).
32. K. Tounai, H. Tanabe, H. Nozue, and K. Kasama, "Resolution improvement with annular illumination," in *Optical/Laser Microlithography V, Proc. SPIE 1674*, 753–764 (1992).
33. D. C. Flanders and H. I. Smith, "Spatial period division exposing," U.S. Patent No. 4,360,586 (Nov. 23, 1982). See claim #8.
34. K. Nakagawa, M. Taguchi, and T. Ema, "Fabrication of 64MB DRAM with *i*-line phase-shift lithography," in *Proc. IEDM*, pp. 817–820 (1990).
35. H. Ohtsuka, K. Abe, T. Onodera, K. Kuwahara, and T. Taguchi, "Conjugate twin-shifter for the new phase shift method to high resolution lithography," in *Optical/Laser Microlithography IV, Proc. SPIE 1463*, 112–123 (1991).
36. H. Jinbo and Y. Yamashita, "0.2  $\mu\text{m}$  of less *i*-line lithography by phase-shifting-mask technology," in *Proc. IEDM*, pp. 825–828 (1990).
37. C. A. Mack, "Fundamental issues in phase-shifting mask technology," in *Proc. KTI Microlithography Seminar*, pp. 23–35 (1991).
38. F. Hurter and V. C. Driffield, "Photo-chemical investigations and a new method of determination of the sensitivity of photographic plates," *J. Soc. Chem. Ind.*, pp. 455–469 (May 31, 1890).
39. C. A. Mack, "Lithographic optimization using photoresist contrast," in *Proc. KTI Microlithography Seminar*, pp. 1–12 (1990); *Microelectron. Manufac. Technol.* **14**(1), 36–42 (1991).



**Chris A. Mack** received BS degrees in physics, chemistry, electrical engineering, and chemical engineering from Rose-Hulman Institute of Technology in 1982 and an MS degree in electrical engineering from the University of Maryland in 1989. He joined the Microelectronics Research Laboratory of the Department of Defense in 1983 and began work in optical lithography research. He has authored numerous papers in the area of optical lithography, regularly teaches courses on this topic, and has developed the lithography simulation programs PROLITH and PROLITH/2. During 1990 to 1991 he was on assignment at SEMATECH working in deep-UV photoresist characterization and phase-shifting mask optimization. Since January 1992 he has been vice-president of research and development for FINLE Technologies and also serves as an adjunct faculty at the University of Texas at Austin. His current interests are advanced optical techniques for ultrafine lithography and the applications of lithography simulation to research, development, and manufacturing.